

$\rho(770)^0$, $K^*(892)^0$ and $f_0(980)$ Production in Au-Au and pp Collisions at $\sqrt{s_{NN}} = 200$ GeV

P. Fachini^a for the STAR Collaboration*

^aBrookhaven National Laboratory, Bldg. 510A, Upton, NY 11973, USA

Preliminary results on $\rho(770)^0 \rightarrow \pi^+\pi^-$, $K^*(892)^0 \rightarrow \pi K$ and $f_0(980) \rightarrow \pi^+\pi^-$ production using the mixed-event technique are presented. The measurements are performed at mid-rapidity by the STAR detector in $\sqrt{s_{NN}} = 200$ GeV Au-Au and pp interactions at RHIC. The results are compared to different measurements at various energies.

1. Introduction

The measurement of resonances that have lifetimes smaller than, or comparable to, the lifetime of the dense matter produced in relativistic heavy-ion collisions provides an important tool for studying the collision dynamics. Resonances that decay before kinetic freeze-out may not be reconstructed due to the re-scattering of the daughter particles. Therefore, short-lived resonance production may provide information on the time between chemical and kinetic freeze-out. The measurement of resonances helps constraining thermal models via their feed-down to stable hadrons and their ratios to other particles [1]. In addition, the measurement of $\rho(770)^0 \rightarrow \pi^+\pi^-$ production can provide information for studying the di-lepton decay channel, since the $\rho(770)^0 \rightarrow \ell^+\ell^-$ production in the hadronic ‘cocktail’ is currently based on model calculations [2]. First results on $\rho(770)^0$, $K^*(892)^0$ and $f_0(980)$ measurements via their hadronic decay channel in Au-Au and pp collisions at $\sqrt{s_{NN}} = 200$ GeV using the STAR detector at RHIC are presented. The results are compared to the measurements in Au-Au, pp, $\bar{p}p$ and e^+e^- interactions at various energies.

2. Data Analysis and Results

The main STAR detector consists of a large Time Projection Chamber (TPC) [3] placed inside an uniform solenoidal magnetic field of 0.5 T. The TPC provides the measurement of charged particles. About 2M Au-Au minimum bias events and about 4.7M pp events at $\sqrt{s_{NN}} = 200$ GeV are used in this analysis. The $\rho(770)^0$, $K^*(892)^0$ and $f_0(980)$ measurements follow our previous $K^*(892)^0$ measurement at $\sqrt{s_{NN}} = 130$ GeV [4]. Due to limited statistics, the term K^{*0} in this analysis refers to the average of K^{*0} and \bar{K}^{*0} unless specified.

The $\pi^+\pi^-$ invariant mass distributions after background subtraction for the 40% to 80% of the hadronic Au-Au cross section and for pp interactions are shown in Fig. 1. The

*For the full author list and acknowledgements, see Appendix ‘‘Collaborations’’ of this volume.

K_S^0 is fit to a gaussian (dotted line), the ω shape (dash-dotted line) is obtained from the HIJING event generator, the K^{*0} shape (dark grey line) is also obtained from HIJING with the kaon being misidentified as a pion, and both the ρ^0 (dashed line) and the f_0 (light grey line) are fit to a Breit-Wigner function with a fixed width of 150 MeV and 75 MeV, respectively. In the case of the ρ^0 and f_0 line shapes, we are investigating distortions due to final state interactions and production via re-scattering. The ω signal is a free parameter in the fit and the K^{*0} signal is fixed according to the $K^*(892)^0 \rightarrow \pi K$ measurement. The solid black line corresponds to sum of all these correlations in the $\pi^+\pi^-$ channel. Since the identification of the daughter particles from the resonance decay is obtained by the energy loss in the gas of the TPC, particle misidentification increases with p_T . As a consequence, the K^{*0} contamination in the $\pi^+\pi^-$ channel limits the measured p_T range of the ρ^0 .

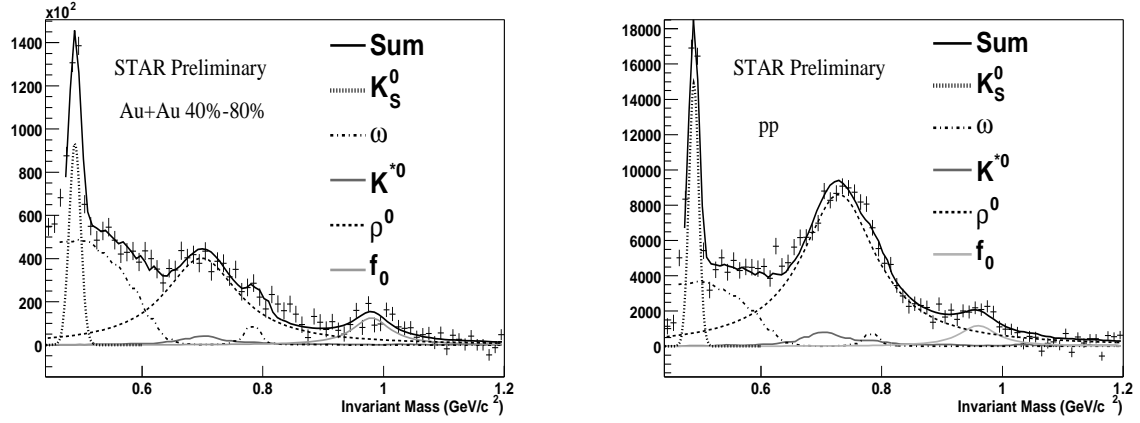


Figure 1. The $\pi^+\pi^-$ invariant mass distributions after background subtraction for the 40% to 80% of the hadronic Au-Au cross section (left) and for pp interactions (right).

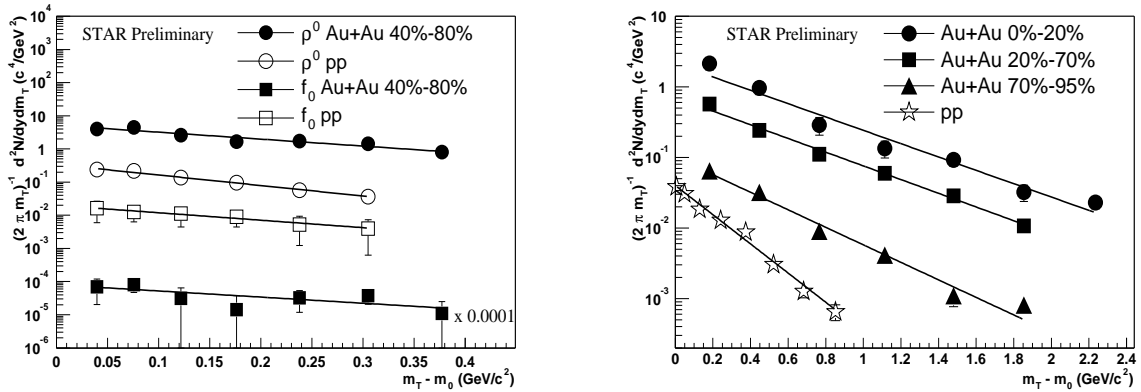


Figure 2. m_T -distributions at mid-rapidity ($|y| < 0.5$) for ρ^0 , f_0 (left) and $(K^{*0} + \overline{K^{*0}})/2$ (right) from Au-Au and pp interactions. The errors shown are statistical only.

In the case of the $K\pi$ invariant mass distribution after background subtraction, a com-

bination of a linear background and a Breit-Wigner function are used to fit the K^{*0} signal with the nominal resonance width and mass, as described in [4].

The ρ^0 , f_0 and $(K^{*0} + \overline{K^{*0}})/2$ m_T -distributions at mid-rapidity ($|y| < 0.5$) from both Au-Au and pp interactions are shown in Fig. 2. An exponential fit is used to extract the yields per unit of rapidity and the inverse slopes. The systematic uncertainty in the K^{*0} dN/dy is estimated to be 25% for Au-Au and 10% for pp collisions due to detector effects and the uncertainty in the background determination. The systematic uncertainty in the ρ^0 and f_0 dN/dy is estimated to be 30% and 50%, respectively for both pp and Au-Au collisions. The measurements from pp interactions are not corrected for trigger bias and vertex finding efficiency. However, these corrections may cancel in the particle ratios.

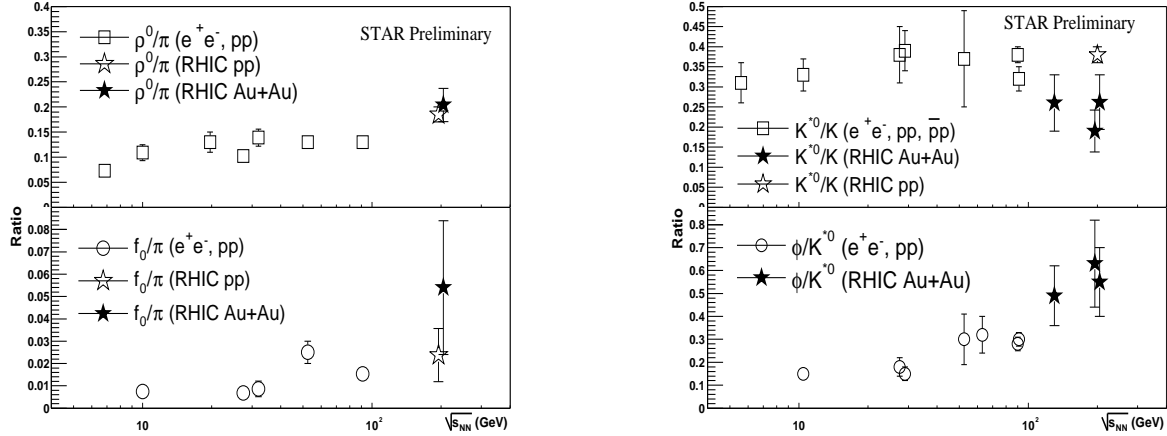


Figure 3. ρ^0/π , f_0/π (left), K^{*0}/K and ϕ/K^{*0} (right) ratios as a function of beam energy. The ρ^0/π and f_0/π ratios from Au-Au collisions correspond to 40-80% of the hadronic cross-section. The K^{*0}/K and ϕ/K^{*0} ratios from Au-Au collisions at $\sqrt{s_{NN}}=200$ GeV correspond to 0-20% and 20-70% of the hadronic cross-section. The ratios are from measurements in e^+e^- collisions at 10.45 GeV [5], 29 GeV [6], 90 GeV [7] and 91 GeV [8] beam energies, $\bar{p}p$ at 5.6 GeV [9] and pp at 6.8 GeV [10], 19.7 GeV [11], 27.5 GeV [12], 52.5 GeV [13] and 63 GeV [14]. The errors on the K^{*0}/K and ϕ/K^{*0} ratios at $\sqrt{s_{NN}}=200$ GeV correspond to the quadratic sum of the statistical and systematic errors. The errors on the other ratios at $\sqrt{s_{NN}}=200$ GeV are statistical only.

In the ρ^0 analysis, we follow previous e^+e^- and pp measurements that do not select exclusively on the $\ell=1$ $\pi^+\pi^-$ channel. Figure 3 depicts the ρ^0/π and f_0/π ratios as a function of beam energy for different colliding systems. Both ρ^0 and f_0 production measured at RHIC seem to follow the trend of previous measurements.

Figure 3 also shows the K^{*0}/K and ϕ/K^{*0} ratios measured in different colliding systems at various energies. The K^{*0}/K ratio is interesting because K^{*0} and K have similar quark content and differ mainly in mass and spin. From Fig. 3, the K^{*0}/K ratio from $\sqrt{s_{NN}}=200$ GeV Au-Au collisions is lower than the pp measurement at the same energy by a factor of 2.

The ϕ/K^{*0} ratio measures the strangeness suppression in nearly ideal conditions since

$\Delta S = 1$, since strangeness is hidden in the ϕ , and there is only a small mass difference. Fig. 3 shows an increase of the ratio ϕ/K^{*0} measured in Au-Au collisions compared to the measurements in pp and e^+e^- at lower energies. However, this increase may not be solely related to strangeness suppression due to additional effects on short lived resonances in heavy-ion collisions.

The K^{*0} lifetime is short ($c\tau = 4$ fm) and comparable to the time scale of the evolution of the system in relativistic heavy-ion collisions. If the K^{*0} decay between chemical and kinetic freeze-out, the daughters from the decay may re-scatter and the K^{*0} will not be reconstructed. On the other hand, elastic interactions are still effective after chemical freeze-out [15] and may regenerate the K^{*0} until kinetic freeze-out. Assuming that the difference in the K^{*0}/K ratio measured in $\sqrt{s_{NN}} = 200$ GeV Au-Au and pp collisions is due to the K^{*0} survival probability, our measurement is consistent with a time of only a few fm between chemical and kinetic freeze-out (scenario [16]). Hence, our measurement at RHIC is consistent with either a sudden freeze-out with no K^{*0} regeneration or a long time scenario (~ 20 fm [17]) with significant K^{*0} regeneration.

3. Conclusions

Preliminary results on $\rho(770)^0$, $K^*(892)^0$ and $f_0(980)$ production measured at mid-rapidity by the STAR detector in $\sqrt{s_{NN}} = 200$ GeV hadronic Au-Au and pp interactions at RHIC were presented. The data show significant production of these short-lived resonances. The K^{*0} production at RHIC rules out a long expansion time between chemical and kinetic freeze-out unless there is significant K^{*0} regeneration, due to elastic interactions after chemical freeze-out. Finally, the study of short-lived resonances may provide important information on the collision dynamics.

REFERENCES

1. G. Van Buren, These Proceedings.
2. J. Kapusta, These Proceedings.
3. H. H. Ackermann *et.al.*, Nucl. Phys. A 661 (1999) 681.
4. C. Adler *et.al.*, nucl-ex/0205015.
5. H. Albrecht *et.al.*, Z. Phys. C 61 (1994) 1.
6. M. Derrick *et.al.*, Phys. Lett. B 158 (1985) 519.
7. K. Abe *et.al.*, Phys. Rev. D 59 (1999) 052001.
8. Y. J. Pei *et.al.*, Z. Phys. C 72 (1996) 39.
9. J. Canter *et.al.*, Phys. Rev. D 20 (1979) 1029.
10. V. Blobel *et.al.*, Phys. Lett. B 48 (1974) 73.
11. R. Singer *et.al.*, Phys. Lett. B 60 (1976) 385.
12. M. Aguilar-Benitez *et.al.*, Z. Phys. C 50 (1991) 405.
13. D. Drijard *et.al.*, Z. Phys. C 9 (1981) 293.
14. T. Akesson *et.al.*, Nucl. Phys. B 203 (1982) 27.
15. H. Bebie *et.al.*, Nucl. Phys. B 378 (1992) 95; R. Rapp and E. V. Shuryak, Phys. Rev. Lett.86 (2001) 2980; C. Song and V. Koch Phys. Rev. C 55 (1997) 3026.
16. G. Torrieri and J. Rafelski, Phys. Lett. B 509(2001) 239.
17. L. V. Bravina *et.al.*, hep-ph/0010172; D. Teaney D *et.al.*, nucl-th/0110037.